Temporal-imaging system with simple external-clock triggering

Daniel H. Broaddus[1,*], Mark A. Foster[1], Onur Kuzucu[1], Amy C. Turner-Foster[2], Karl W. Koch[3], Michal Lipson[2], and Alexander L. Gaeta[1]

[1]*School of Applied and Engineering Physics, Cornell University, Ithaca, NY 14853 USA*
[2]*School of Electrical and Computer Engineering, Cornell University, Ithaca, NY 14853 USA*
[3]*Corning Incorporated, Corning, NY 14831 USA*
**dhb29@cornell.edu*

Abstract: We demonstrate a temporal imaging system based on parametric mixing that allows simple triggering from an external clock by using a time-lens-based pump laser. We integrate our temporal imaging system into a time-to-frequency measurement scheme and demonstrate the ability to perform characterization of temporal waveforms with 1.4-ps resolution and a 530-ps record length. We also integrate our system into a temporal-magnification scheme and demonstrate single-shot operation with a 113 × magnification factor, 1.5-ps resolution, and 220-ps record length.

OCIS codes: (320.7100) Ultrafast measurements; (130.3120) Integrated optics devices.

References and links

1. E. Treacy, "Optical pulse compression with diffraction gratings," IEEE J. Quantum Electron. **5**(9), 454–458 (1969).
2. S. A. Akhmanov, V. A. Vysloukh, and A. S. Chirkin, "Self-action of wave packets in a nonlinear medium and femtosecond laser pulse generation," Sov. Phys. Usp. **29**(7), 642–647 (1986).
3. B. H. Kolner, and M. Nazarathy, "Temporal imaging with a time lens," Opt. Lett. **14**(12), 630–632 (1989).
4. B. H. Kolner, "Space-time duality and the theory of temporal imaging," IEEE J. Quantum Electron. **30**(8), 1951–1963 (1994).
5. C. Bennett, and B. Kolner, "Principles of parametric temporal imaging—Part I. System configurations," IEEE J. Quantum Electron. **36**(4), 430–437 (2000).
6. R. Salem, M. A. Foster, A. C. Turner, D. F. Geraghty, M. Lipson, and A. L. Gaeta, "Optical time lens based on four-wave mixing on a silicon chip," Opt. Lett. **33**(10), 1047–1049 (2008).
7. L. Mouradian, F. Louradour, V. Messager, A. Barthelemy, and C. Froehly, "Spectro-temporal imaging of femtosecond events," IEEE J. Quantum Electron. **36**(7), 795–801 (2000).
8. Y. Han, O. Boyraz, and B. Jalali, "Tera-sample per second real-time waveform digitizer," Appl. Phys. Lett. **87**(24), 241116–241118 (2005).
9. C. Dorrer, "Single-shot measurement of the electric field of optical waveforms by use of time magnification and heterodyning," Opt. Lett. **31**(4), 540–542 (2006).
10. C. V. Bennett, and B. H. Kolner, "Upconversion time microscope demonstrating 103 x magnification of femtosecond waveforms," Opt. Lett. **24**(11), 783–785 (1999).
11. R. Salem, M. A. Foster, A. C. Turner-Foster, D. F. Geraghty, M. Lipson, and A. L. Gaeta, "High-speed optical sampling using a silicon-chip temporal magnifier," Opt. Express **17**(6), 4324–4329 (2009).
12. Y. Okawachi, R. Salem, M. A. Foster, A. C. Turner-Foster, M. Lipson, and A. L. Gaeta, "High-resolution spectroscopy using a frequency magnifier," Opt. Express **17**(7), 5691–5697 (2009).
13. M. T. Kauffman, W. C. Banyai, A. A. Godil, and D. M. Bloom, "Time-to-frequency converter for measuring picosecond optical pulses," Appl. Phys. Lett. **64**(3), 270–272 (1994).
14. T. Mansuryan, A. Zeytunyan, M. Kalashyan, G. Yesayan, L. Mouradian, F. Louradour, and A. Barthélémy, "Parabolic temporal lensing and spectrotemporal imaging: a femtosecond optical oscilloscope," J. Opt. Soc. Am. B **25**(6), A101–A110 (2008).
15. P. C. Sun, Y. T. Mazurenko, and Y. Fainman, "Femtosecond pulse imaging: Ultrafast optical oscilloscope," J. Opt. Soc. Am. A **14**(5), 1159–1170 (1997).
16. J.-H. Chung, and A. M. Weiner, "Real-time detection of femtosecond optical pulse sequences via time-to-space conversion in the lightwave communications band," J. Lightwave Technol. **21**(12), 3323–3333 (2003).
17. Y. Takagi, Y. Yamada, K. Ishikawa, S. Shimizu, and S. Sakabe, "Ultrafast single-shot optical oscilloscope based on time-to-space conversion due to temporal and spatial walk-off effects in nonlinear mixing crystal," Jpn. J. Appl. Phys. **44**(No. 9A), 6546–6549 (2005).
18. M. A. Foster, R. Salem, D. F. Geraghty, A. C. Turner-Foster, M. Lipson, and A. L. Gaeta, "Silicon-chip-based ultrafast optical oscilloscope," Nature **456**(7218), 81–84 (2008).

#125692 - $15.00 USD Received 24 Mar 2010; revised 31 May 2010; accepted 1 Jun 2010; published 18 Jun 2010

19. P. J. Almeida, P. Petropoulos, B. C. Thomsen, M. Ibsen, and D. J. Richardson, "All-optical packet compression based on time-to-wavelength conversion," IEEE Photon. Technol. Lett. **16**(7), 1688–1690 (2004).
20. M. A. Foster, R. Salem, Y. Okawachi, A. C. Turner-Foster, M. Lipson, and A. L. Gaeta, "Ultrafast waveform compression using a time-domain telescope," Nat. Photonics **3**(10), 581–585 (2009).
21. J. Chou, C. V. Bennett, O. Boyraz, and B. Jalali, "Triggerable continuum source for single-shot ultra-fast applications," in *Proceedings of IEEE Conference on Lasers and Electro-Optics Society* (Institute of Electrical and Electronics Engineers, New York, 2006), pp. 806–807.
22. D. H. Broaddus, M. A. Foster, O. Kuzucu, A. C. Turner-Foster, M. Lipson, and A. L. Gaeta, "Temporal Imaging System with Simple External Clock Synchronization," in *Conference on Lasers and Electro-Optics/International Quantum Electronics Conference*, OSA Technical Digest (CD) (Optical Society of America, 2009), paper CFK3.
23. A. C. Turner, M. A. Foster, A. L. Gaeta, and M. Lipson, "Ultra-low power parametric frequency conversion in a silicon microring resonator," Opt. Express **16**(7), 4881–4887 (2008).
24. M. A. Foster, A. C. Turner, J. E. Sharping, B. S. Schmidt, M. Lipson, and A. L. Gaeta, "Broad-band optical parametric gain on a silicon photonic chip," Nature **441**(7096), 960–963 (2006).
25. Y. H. Kuo, H. Rong, V. Sih, S. Xu, M. Paniccia, and O. Cohen, "Demonstration of wavelength conversion at 40 Gb/s data rate in silicon waveguides," Opt. Express **14**(24), 11721–11726 (2006).
26. Q. Lin, J. Zhang, P. M. Fauchet, and G. P. Agrawal, "Ultrabroadband parametric generation and wavelength conversion in silicon waveguides," Opt. Express **14**(11), 4786–4799 (2006).
27. A. C. Turner, C. Manolatou, B. S. Schmidt, M. Lipson, M. A. Foster, J. E. Sharping, and A. L. Gaeta, "Tailored anomalous group-velocity dispersion in silicon channel waveguides," Opt. Express **14**(10), 4357–4362 (2006).
28. J. van Howe, and C. Xu, "Ultrafast optical signal processing based upon space-time dualities," IEEE J. Lightwave Technol. **24**(7), 2649–2662 (2006).
29. D. R. Solli, C. Ropers, P. Koonath, and B. Jalali, "Optical rogue waves," Nature **450**(7172), 1054–1057 (2007).
30. J. Azaña, and M. Muriel, "Real-time optical spectrum analysis based on the time-space duality in chirped fiber gratings," IEEE J. Quantum Electron. **36**(5), 517–526 (2000).
31. Y. Han, and B. Jalali, "Photonic time-stretched analog-to-digital converter: fundamental concepts and practical considerations," IEEE J. Lightwave Technol **21**(12), 3085–3103 (2003).
32. V. J. Hernandez, C. V. Bennett, B. D. Moran, A. D. Drobshoff, C. Langrock, D. Chang, M. M. Fejer, and M. Ibsen, "745 fs Resolution Single-Shot Recording at 2.1 Tsample/s and 104 Mframes/s Using Temporal Imaging," in *Nonlinear Optics: Materials, Fundamentals and Applications*, OSA Technical Digest (CD) (Optical Society of America, 2009), paper PDNFA2.
33. S. V. Chernikov, J. R. Taylor, P. V. Mamyshev, and E. M. Dianov, "Generation of soliton pulse train in optical fibre using two CW singlemode diode lasers," Electron. Lett. **28**(10), 931–932 (1992).

1. Introduction

The demand for ultrafast-pulse characterization and waveform-generation techniques has driven research for high-bandwidth characterization systems. This has led to the development of temporal-imaging and dispersion-based techniques that exploit the space-time duality of electromagnetic fields [1–6]. Techniques such as time stretching [7–9], time magnification [10,11], frequency magnification [12], time-to-frequency conversion [13,14], time-to-space conversion [15–18], pulse compression [5], and ultrafast-waveform compression [19,20] have been demonstrated. Recent implementations [6,11,12,17,19] based on a four-wave mixing (FWM) time-lens require synchronized pump and signal pulses. This is achieved by extracting the pump and the signal from the same source by spectral filtering. Conversely, using a separate mode-locked fiber laser would provide the necessary bandwidth for ultrafast temporal imaging, but would require repetition-rate locking using a feedback loop to achieve synchronous operation. Ultimately, either of these schemes is restricted by the types of signal that can be measured. Therefore, it is desirable to develop a system in which high bandwidth pump pulses can be produced on-demand via a simple external trigger [21,22].

In this paper, we propose and demonstrate a fully triggerable temporal-imaging system. We base our system on a time-lens-compressed picosecond pulse source. The output of the pulsed time-lens source is then spectrally broadened in non-zero dispersion-shifted fiber through self-phase modulation (SPM), which provides the pulses with sufficient bandwidth for ultrafast temporal imaging with high temporal resolution. We characterize the performance of our pulsed source by integrating it into a time-lens-based ultrafast optical oscilloscope (UFO), which uses time-to-space conversion, to demonstrate multi-shot time-averaged wavepacket measurement. We also characterize our system in a temporal-magnification scheme to perform high-temporal-resolution single-shot measurements. We demonstrate the ability to characterize arbitrary waveforms with 1.4-ps resolution with 530-ps

#125692 - $15.00 USD Received 24 Mar 2010; revised 31 May 2010; accepted 1 Jun 2010; published 18 Jun 2010

record length in multi-shot configuration and 1.5-ps resolution and 220-ps record length in single-shot configuration.

2. Theory

Temporal-imaging systems are based on the space-time duality. Similar to a spatial-lens that imparts a quadratic spatial phase across the beam, a time-lens imparts a temporal quadratic phase across a pulse [1–6]. In previous demonstrations, the required quadratic phase for a time-lens was typically applied by an electro-optic phase modulator [13]. In parametric temporal imaging, nonlinear optical (NLO) processes replace electro-optic phase modulators as the source of phase modulation [4–6]. In a parametric time-lens, a pump pulse with a quadratic temporal phase is mixed with a signal pulse in either a $\chi^{(2)}$ or $\chi^{(3)}$ parametric process to impart a quadratic-phase shift on the converted pulse. Since a quadratic-phase shift is equivalent to a linear frequency chirp, sending a broadband pump pulse through a dispersive fiber link can impart the desired quadratic temporal phase on the signal. Additionally, in a time-lens, the analog to an aperture is the temporal duration of the pulse. Therefore, to ensure the pump pulse gives equal weight to all temporal components, a spectrally flat pump pulse is desired.

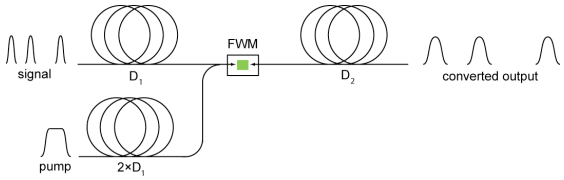

Fig. 1. Schematic of a FWM-based time-lens system. A signal sent through an optical fiber with the group-delay dispersion matching the focal length of the time-lens is mixed with a linearly chirped pump pulse in a FWM process. The converted output experiences a quadratic phase shift. In this case, the output would undergo time-magnification by a factor of D_2/D_1, where D_1 and D_2 are the group velocity dispersion (GVD) parameters for the fiber before and after the FWM interaction, respectively.

FWM in silicon offers low pump-power requirements [23] and a large conversion bandwidth that is suitable for high data-rate applications [24–27]. In addition, in FWM-based time-lens systems the signal and converted wavelengths can be close together, allowing them to be amplified, guided, and detected by similar equipment. Figure 1 shows a schematic of a FWM-based time-lens. However, recent time-lens systems [6,11,12,17,20] lack an adaptable pump source necessary for the measurement capability of signal inputs that are independently generated from the pump. Ideally, such a source would be fiber coupled, spectrally flat, and capable of producing high-bandwidth pulses on demand.

3. Experiment

In order to create a suitable, triggerable pump pulse, we use a time-lens-compressed picosecond-pulse source [21,22,28]. Unlike conventional ultrafast laser sources, the time-lens source derives its repetition rate from an input RF signal rather than an oscillator cavity. This makes the source ideal for synchronization, since the laser can be synchronized to a clock signal from any source as its input. Although this system cannot be driven at an arbitrarily low repetition rate, we can select a harmonic of the input clock between 5 and 10 GHz that will allow for optimal operation of the system while still providing a synchronized pump pulse for every signal pulse. At repetition rates above 10 GHz, electronic filtering can be used to generate a suitable drive signal from the input clock. We obtain the clock signal from a photodetector output of a test laser. The clock signal drives an amplitude modulator that carves out pulses from a tunable cw source resulting in a 33% duty cycle pulse train. We send this output through an EDFA and then filter out the background amplified spontaneous emission. We apply a quadratic phase across the pulses by using a 10-GHz electro-optic phase modulator, which is driven by a harmonic of the input clock. The pulses propagate through

#125692 - $15.00 USD Received 24 Mar 2010; revised 31 May 2010; accepted 1 Jun 2010; published 18 Jun 2010

1.6 km of SMF-28 fiber, which compresses the pulses to roughly 4.5 ps in duration. Figure 2 shows a diagram of the time-lens source.

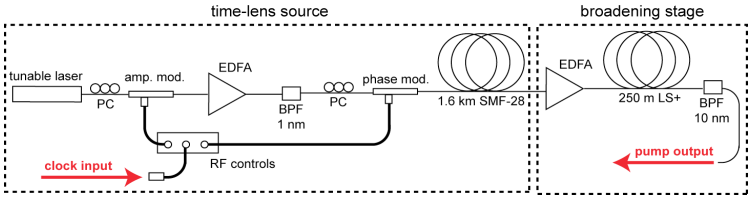

Fig. 2. Schematic of the pump source. Pulses are generated using an arbitrary RF clock input, and then spectrally broadened through SPM in a low normal-dispersion fiber.

Achieving fine resolution and long record lengths in temporal imaging systems requires sufficiently high pump bandwidth. At the output of the time-lens source, the pulses have a bandwidth of 1 nm centered at 1546 nm. To increase the bandwidth, we add a spectral broadening stage to the pump source after the time-lens compression stage. After passing the pulses through another EDFA, we send them through 250 m of Corning® Vascade® LS + fiber. The pulses undergo SPM and see an increase in bandwidth from 1 nm to 100 nm. We filter a spectrally flat off-center section of the output roughly 10 nm in bandwidth at 1559 nm to serve as the pump pulse. After the broadening stage, we note a large amplitude noise at the output for high input intensities [27]. In order to maintain a suitable pump output, we limit the pulse energy at the input of the Corning® Vascade® LS + fiber to 2 nJ.

4. Results

As a proof-of-concept demonstration, we integrate this pulse source into a silicon-time-lens based UFO [13–17]. The goal of this demonstration is to show the viability of our temporal-imaging system for use in a variety of time-lens-based applications. In this scheme, the silicon time-lens works as a Fourier transforming device, and temporal information is directly converted to the spectral domain. We can then view the temporal profile of the pulse on an optical spectrum analyzer (OSA) trace. We linearly chirp the pump pulse by sending it through a pair of fibers, a dispersion compensation fiber (DCF) and a length of Corning® Vascade® S1000 fiber, with a total of −50 ps/nm of group-delay dispersion. Taking advantage of their opposite dispersion slopes, we pair the fibers' lengths to achieve low third-order dispersion (TOD). We characterize a sub-picosecond signal pulse created by filtering 10 nm of spectrum from the output of a mode-locked fiber laser.

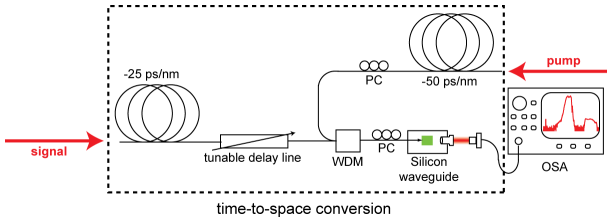

Fig. 3. A schematic of the UFO scheme. The signal undergoes half as much dispersion as the pump, which corresponds to the focal length of the time-lens. The pump and the signal mix on the silicon waveguide. An OSA displays the output spectrum of both inputs and the idler output, and the idler spectrum emerges as a scaled version of the signal input in time domain.

We pick off another portion of the fiber laser output and feed it into a photodiode. The output of the photodiode serves as the clock input to our pump laser. We send the fiber laser pulse through −25 ps/nm of dispersion, which corresponds to the focal length of the silicon-time-lens. Again, we utilize a combination of DCF and Corning® Vascade® S1000 fiber to achieve low TOD. Figure 3 shows a detailed layout of the UFO. We combine the two pulses and overlap them in time, and couple the combined output into a silicon waveguide for FWM.

#125692 - $15.00 USD Received 24 Mar 2010; revised 31 May 2010; accepted 1 Jun 2010; published 18 Jun 2010

The waveguide is 300 nm by 700 nm and 1.5 cm in length, which is optimal for broadband FWM [24,27].

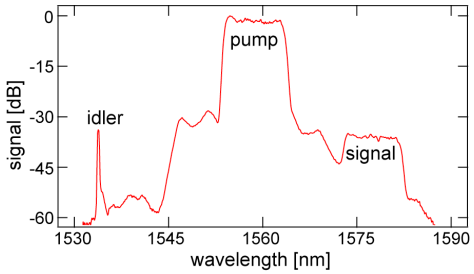

Fig. 4. The pump and signal pulses mix to form a narrowband idler. The flat spectral profile of the pump ensures fidelity over the entire aperture of the time-lens.

Monitoring the output spectrum on an OSA, we vary the signal pulse delay to calibrate our system. We find a time-to-frequency conversion factor of 0.036 nm/ps, and an average temporal resolution of 1.4 ps over a record length of 530 ps. Figure 4 shows an OSA trace of the FWM output. The broadband pump and signal combine to generate a narrow band idler, which corresponds to an ultrafast signal pulse in the time domain. Figure 5 shows the measured UFO traces as the signal pulse timing is varied. From this measurement, we calculate a record length of 530 ps. Figure 5 (inset) shows the 1.4-ps impulse response of the system.

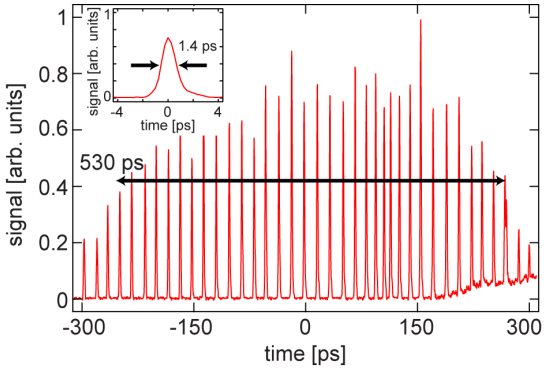

Fig. 5. A composite OSA trace showing the full record length of 530 ps, and a single trace (inset) showing the 1.4-ps resolution of the system.

Next, we investigate the single-shot operation performance of our temporal imaging system by integrating our setup into a temporal-magnification system [10,11]. For this scheme, we launch the signal into a dispersive link with a total group-delay dispersion of 6100 ps/nm, which is comprised of 360 km of SMF28e fiber. Since this large dispersive length can be considered imaging in the Fraunhofer far-field, our converted signal's temporal profile takes on the shape of its spectral profile [30]. The output of the dispersive link is fed into a 12.5-GHz photodiode and viewed on a 5-GHz LeCroy oscilloscope. Figure 6 shows a layout of the temporal imaging system in a single-shot configuration.

#125692 - $15.00 USD Received 24 Mar 2010; revised 31 May 2010; accepted 1 Jun 2010; published 18 Jun 2010

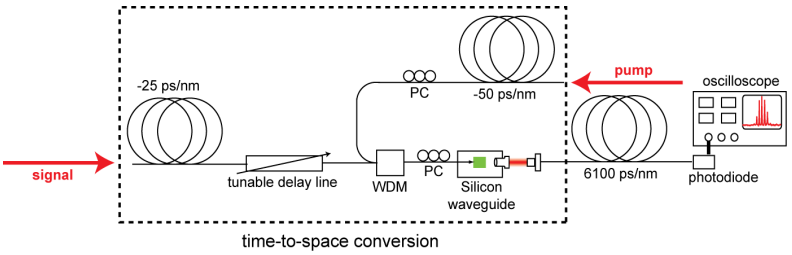

Fig. 6. A schematic of the single-shot temporal-magnification system. The signal undergoes time-to-frequency conversion and is sent through a dispersive fiber link. Analogous to far-field diffraction, the temporal profile of the converted output takes on the spectral profile. This results in the magnification of the initial temporal profile of the signal. A 5-GHz LeCroy oscilloscope displays the photodiode output.

We characterize our system's single-shot performance by temporally resolving the output of a bandpass filtered mode-locked fiber laser, and by varying the delay on the signal showing 1.5-ps resolution over a record length of 220 ps. In addition, we calculate magnification factor to be 113 ×. Figure 7 shows a composite oscilloscope trace showing the timing of the signal pulse as it is varied over the entire record length. Figure 8 shows a blow-up of a single signal pulse demonstrating the temporal resolution of the system. Limited only by the signal repetition rate and magnification factor, the single-shot record length could easily be increased to the full 530 ps by frequency de-multiplexing the output into three channels [31].

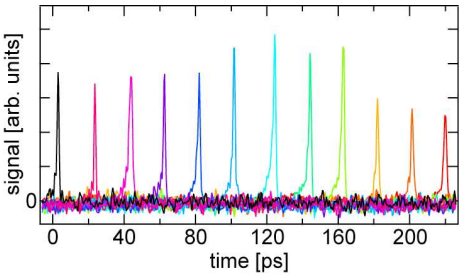

Fig. 7. A composite oscilloscope trace obtained by multiple data acquisitions with varying signal-pump delays showing the single-shot record length of 220 ps.

In addition, we characterize the small time-scale jitter over 2 μs. The experimental configuration allows for high frame rates, which provides the ability to characterize consecutive waveforms [32]. We use this ability to analyze the timing of 77 consecutive pulses from the fiber laser utilizing the sync out for the fiber laser as a timing reference. We find that the root-mean-square (RMS) value of the timing jitter was 0.27 ps over 2-μs measurement period. The histogram in Fig. 8(b) shows the variation in pulse-to-pulse timing. The low RMS value of the jitter suggests that resolution could be further improved. Reducing phase aberrations from higher-order dispersion and the SPM broadening stage would likely yield the desired result.

#125692 - $15.00 USD Received 24 Mar 2010; revised 31 May 2010; accepted 1 Jun 2010; published 18 Jun 2010

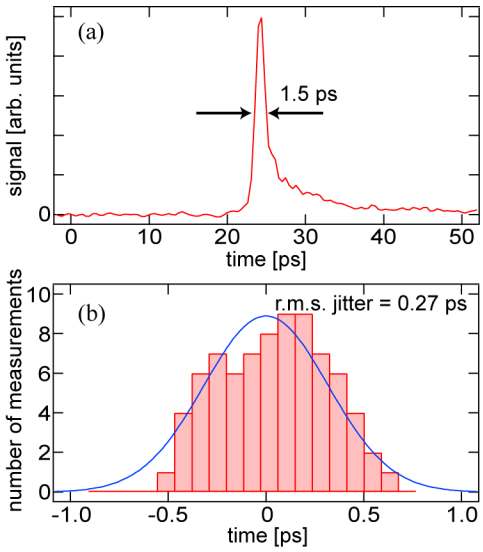

Fig. 8. (a) A plot of an individual pulse showing the impulse response of the temporal-magnification system to be 1.5 ps. The tail on the pulse arises from the response of the photodiode. (b) A histogram of the pulse-to-pulse jitter between the output of the system and the sync output of the fiber laser functioning as the test system. The r.m.s. value of the timing jitter is shown to be 0.27 ps over 2 microseconds.

Finally, to demonstrate that the system is not limited to transform-limited waveforms, we characterize the intensity fringes between two interfering 40-ps laser pulses separated in wavelength but temporally overlapped. To create the pulses, we modulate two cw lasers that are not phase-locked and tune their wavelengths.

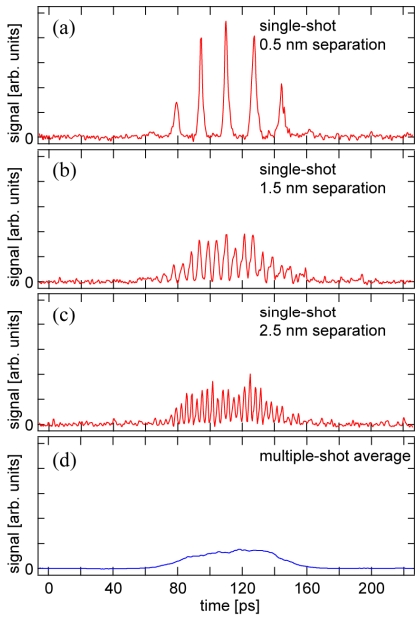

Fig. 9. The fringe period decreases with increasing separation. (a) 0.5 nm separation with movie showing phase procession between the lasers (Media 1). We believe the non-sinusoidal shape of these peaks arises from soliton effect compression in the amplifier before the temporal imaging stage [33]. (b) 1.5 nm separation, and (c) 2.5 nm separation. (d) The phase slip between the two lasers, which are not phase-locked, washes out the fringes when averaged over multiple shots.

#125692 - $15.00 USD Received 24 Mar 2010; revised 31 May 2010; accepted 1 Jun 2010; published 18 Jun 2010

As we increase the wavelength separation of the pulses, the temporal width of the interference fringes decreases. Figure 9 shows the fringe period decreasing with increasing separation. Furthermore, this measurement is inherently single-shot, since the phase relation between the two signal lasers is continuously changing. Single-shot measurements show pronounced fringes, while when averaged over multiple shots, the fringes wash out. Figure 9(d) shows a multi-shot average of the pulse envelope where the fringe contrast disappeared. It is possible to take several successive waveforms and follow the procession of one laser's phase with respect to another, which Media 1 shows for two lasers separated by 0.5 nm and sampled at 40 MHz.

5. Conclusion

We demonstrated a completely triggerable temporal-imaging system. We characterized the system's performance in both multi-shot and single-shot time-lens-based schemes. We showed 1.4 ps resolution with 530 ps record length using time-to-frequency conversion. In a single-shot temporal magnification system, .we demonstrated a 1.5-ps resolution and a 220-ps record length. We also characterized the short-term timing jitter present between our pump and signal pulses and measured it to be 0.27 ps, which corresponds to 18% of the temporal resolution. Finally, we illustrate the ability to perform complex waveform measurements by resolving the interference fringes between two frequency-separated laser pulses.

Acknowledgements

The authors would like to acknowledge the generous material support received from Corning, Incorporated. This research was supported by the DARPA Optical Arbitrary Waveform Generation Program, and by the Cornell Center for Nanoscale Systems through NSF grant number EEC-0117770.

#125692 - $15.00 USD Received 24 Mar 2010; revised 31 May 2010; accepted 1 Jun 2010; published 18 Jun 2010